

Impacts of C₆₀-Ionic Liquids (ILs) Interactions and IL Alkyl Chain Length on C₆₀ Dispersion Behavior: Insights at the Molecular Level

Zhuang Wang,* Lili Tang,[†] and Degao Wang[‡]

Jiangsu Key Laboratory of Atmospheric Environment Monitoring and Pollution Control (AEMPC), School of Environmental Science and Engineering, Nanjing University of Information Science and Technology, Nanjing 210044, P.R. China

*E-mail: zhuang.wang@nuist.edu.cn

[†]Jiangsu Environmental Monitoring Centre, Nanjing 210036, P.R. China

[‡]Department of Environmental Science and Engineering, Dalian Maritime University, Dalian, 116026, P.R. China

Received February 16, 2014, Accepted May 11, 2014

Mechanisms underlying the impacts of interactions between carbon nanoparticles (CNPs) and ionic liquids (ILs) on the physicochemical behavior of CNPs need to be more fully worked out. This manuscript describes a theoretical investigation at multiple levels on the interactions of fullerene C₆₀ with 21 imidazolium-based ILs of varying alkyl side chain lengths and anionic types and their impacts on C₆₀ dispersion behavior. Results show that π -cation interaction contributed to mechanism of the C₆₀-IL interaction more than π -anion interaction. The calculated interaction energy (E_{INT}) indicates that C₆₀ can form stable complex with each IL molecule. Moreover, the direction of charge transfer occurred from IL to C₆₀ during the C₆₀-IL interaction. Quantitative models were developed to evaluate the self-diffusion coefficient of C₆₀ ($D_{\text{fullerene}}$) in bulk ILs. Three interpretative molecular descriptors (heat of formation, E_{INT} , and charge) that describe the C₆₀-IL interactions and the alkyl side chain length were found to be determinants affecting $D_{\text{fullerene}}$.

Key Words : Fullerene, Ionic liquids, Interaction, Dispersion, Molecular modeling

Introduction

Carbon nanoparticles (CNPs) which are likely to be released to the environment as the result of a variety of human-related sources (release from polymeric products and/or direct discharge to surface water, *etc.*) move across environmental boundaries, and may thus end up in most media.¹⁻³ To appropriately evaluate the potential environmental risks posed by CNPs, it is crucial to understand critical physicochemical processes affecting the behavior of CNPs after release.^{4,5} Physicochemical interactions are of particular concern, as CNPs with high surface reactivity can interact with a variety of compounds in the aquatic environment, such as natural organic matter,^{6,7} surfactants,^{8,9} and environmentally relevant organic acids.¹⁰ Numerous studies have attempted to address the effects of these interactions on the surface properties,¹¹ aggregation/deposition¹² and dispersion behavior,¹³ as well as ecotoxicities of CNPs.¹⁴

Ionic liquids (ILs) are a new class of organic salts that are composed solely of cations and anions.¹⁵ ILs can promise enormous potential for industrial applications, due to their unusual low melting temperature, relatively low viscosity, negligible vapor pressure, as well as high thermal and chemical stability.¹⁶ Moreover, contemporary studies indicate that their “greenness” depends strongly on their structures,¹⁷ and that these intrinsic properties also make ILs superior as ideal dispersing media for CNPs.¹⁸⁻²⁰ Accordingly, it is presently unclear whether CNPs produced in the presence of ILs will directly correspond to CNP-IL complexes that will be found in the environment. Furthermore, though there is

no direct evidence for ILs being found in the environment, recent efforts to prepare for possible release suggest that ILs can present a low to high risk to human and ecological species.^{16,21,22} However, very little information is available on the impacts of CNP-IL interactions on the physicochemical behavior of CNPs. This is due to the fact that experimental data about the interactions between CNPs and ILs are not readily available, and the mechanisms underlying the interactions need to be more fully worked out. Therefore, we should start by focusing on the particular interaction when the combined exposure to CNPs and ILs is being evaluated.

Experimental testing for the physicochemical interactions of CNPs can be laborious, costly, and time-consuming. Current computational methods such as molecular modeling has emerged in recent years as an important complement to experiment for delivering useful information on molecular properties and providing an insight to the interaction mechanisms of CNPs with other compounds from the environment.²³⁻²⁶ Because of its well-defined structure, C₆₀ was frequently chosen as a representative CNP in computational studies assessing the physicochemical interactions of CNPs.^{24,25} It was the purpose of this study to investigate the interactions between C₆₀ and 21 imidazolium-based ILs containing various alkyl side chain lengths and anionic types by molecular modeling. Optimum molecular geometry corresponding to the strongest binding of C₆₀ with each IL was assessed by molecular mechanics (MM) simulations. The radial distribution function (RDF) $g(r)$ of the selected atoms of the IL-cation or anion to the centre of mass of C₆₀ was calculated to understand the interaction mechanism. Quantum

mechanics (QM) approaches were devoted to the estimation of heat of formation (HF) and interaction energy (E_{INT}) of C_{60} with ILs, which were utilized to evaluate the formation and stability of the IL- C_{60} complexes, respectively. Charge transfer was elucidated during the C_{60} -IL interaction. Later, we also described the microscopic dispersion process of C_{60} agglomerates in bulk ILs by large-scale molecular dynamics (MD) simulations. On the basis of the mechanism understanding, linear regression models for the quantitative assessment of the self-diffusion coefficient of C_{60} ($D_{\text{fullerene}}$) in bulk ILs consisting of quantum chemical parameters and number of carbon atoms in the alkyl chain (n_C) were developed using partial least squares (PLS) technique.

Computational Methods

Theoretical Methods. In this study, seven homologues of imidazolium-based ILs ($[C_n\text{mim}]^+$) paired to three different anions (tetrafluoroborate $[\text{BF}_4]^-$, chloride $[\text{Cl}]^-$, and hexafluorophosphate $[\text{PF}_6]^-$) were selected as model molecules (Figure 1). To find the best geometry for each C_{60} -IL complex, a classical annealing simulation was carried out using the Forcite Plus code.²⁷ The universal force field was adopted to perform this simulation. The cutoff radius was chosen to be 18.5 Å. The annealing simulation was carried out as follows: a total of 200 annealing cycles was simulated with an initial (mid cycle) temperature of 200 K (300 K) and 50 heating ramps per cycle, with 100 dynamic steps per ramp. The canonical ensemble (NVT) was used, and the molecular dynamics were performed with a time step of 1.0 fs and a Nose' thermostat. After each cycle, the lowest energy configuration was optimized. The atomic configuration with the lowest total energy for each C_{60} -IL complex was built as a set of inputs for the calculations of quantum chemical properties. Meanwhile, the annealing simulation was also carried out in a $20 \text{ \AA} \times 20 \text{ \AA} \times 20 \text{ \AA}$ unit cell consisting of each optimized C_{60} -IL complex for the RDF calculations.

The quantum chemical calculations of HF and total energy (E_T) have been carried out at the semi-empirical level of the theory with use of MOPAC-PM3 method in the ChemOffice software (Ver. 11.0). Semi-empirical methods are usually much faster with the comparison of ab initio and density

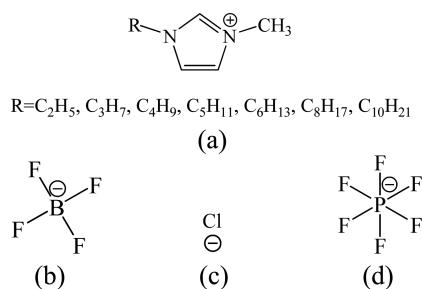


Figure 1. Schematic diagram showing the ionic liquids (ILs) studied in this work. Cations: (a) seven homologues of imidazolium-based ILs; Anions: (b) tetrafluoroborate, (c) chloride, and (d) hexafluorophosphate.

functional theory calculations, enable to perform calculations for larger systems.²⁸ Mulliken population analysis as a probe of elucidating charge transfer during the C_{60} -IL interaction was performed at the same level of theory on the optimized structures.

The bulk ILs and C_{60} -IL dispersions were molded using full atomistic MD simulations in NVT ensemble using the universal force field,¹⁸ subjected to periodic boundary conditions in all three directions. The IL bulk phase consisted of 250 pairs of IL-cations and IL-anions in a $45 \text{ \AA} \times 45 \text{ \AA} \times 45 \text{ \AA}$ unit cell. The initial configuration of the C_{60} -IL system consisted of an agglomerate species of C_{60} and the IL phase. Our MD simulations were performed at the temperature of 298 K. A simulation step of 100,000 was carried out to relax the system into equilibrium at a time step of 0.1 fs and the final one 10 ps for production. As shown in Figure S1 (Supplementary data), the system has already achieved equilibrium after the simulation time. MD simulations have been carried out using Material Explorer 5.0 program.

Radial Distribution Function Calculation and Interaction Energy. RDF that indicates the density change of microscopic atoms or molecules as function of the distance from one particular atom or molecule was employed to elucidate the feature of the C_{60} -IL interaction. RDF was calculated by:

$$g(r) = \frac{dN}{\rho 4\pi r^2} \quad (1)$$

where $g(r)$ is the RDF, dN is the number of atoms or molecules at a distance between r and $r + dr$ from a given target atom or molecule, ρ is the density of the studied system.

E_{INT} was used to evaluate the stability of the C_{60} -IL complexes. The magnitude of E_{INT} is an indication of the magnitude of the driving force towards complexation. The more negative the E_{INT} value, the more thermodynamically favorable the inclusion complex is. E_{INT} was calculated as follows:

$$E_{\text{INT}} = E_T(C_{60} + \text{IL}) - E_T(C_{60}) - E_T(\text{IL}) \quad (2)$$

where $E_T(C_{60} + \text{IL})$, $E_T(C_{60})$, and $E_T(\text{IL})$ represent the optimized E_T of the complex, the isolated C_{60} , and the IL molecules, respectively.

Mean Square Displacement and Self-diffusion Coefficient. The mean square displacement (MSD) that describes the average displacement of an atom during a fixed time t , was employed to characterize the dispersion process of C_{60} in the bulk ILs. The MSD for C_{60} in the bulk ILs was calculated by preparing several time series data items of Length t , averaging those data items, and averaging those data items based on the number of atoms (N), then MSD is defined as follows:

$$\text{MSD} = \langle |r(t) - r(0)|^2 \rangle = \frac{1}{NM} \sum_t \sum_k^M |r_i(t_k + t) - r_i(t_k)|^2 \quad (3)$$

where M is the number of time series data, and t_k is the starting time of k -th time series data. The $D_{\text{fullerene}}$ value was calculated using Einstein's equation:

$$D_{\text{fullerene}} = \frac{1}{6t} MSD \quad (4)$$

The PLS regression was performed with XLSTAT (Ver. 2013.5.03) to construct quantitative models.

Results and Discussion

Features of Interactions between C₆₀ and ILs. The optimized conformations obtained after the annealing simulation are shown in Figure S2 (Supplementary data). The optimized geometries for ILs adsorbed onto the surface of C₆₀ indicate that the IL-cation has a stronger affinity than its anionic partner. Maciel *et al.* also found that in [C₄mim][BF₄] the IL-cation nears the surface of C₆₀ described using an extensive MD simulation.²⁰ To make insight into the structure of ILs around the C₆₀ more deeply, the RDF profiles of nitrogen-2 atom in [C_nmim]⁺, boron atom in [BF₄]⁻, chloride atom in [Cl]⁻, phosphorus atom in [PF₆]⁻ relative to the centre of mass of C₆₀ were characterized (Fig. S3-S5, Supplementary data). The radius of C₆₀ (-3.49 Å) is marked in Figure S3-S5 to indicate the distance between the selected atoms of ILs and the approximate spherical surface of C₆₀. There is an obvious peak near the C₆₀ surface in each RDF curve for the both selected atoms of ILs relative to the C₆₀ centroid. This means that there are π -cation and π -anion interactions between C₆₀ and ILs. For all the 21 ILs studied, it was observed that the RDF peaks for the IL-cations were higher than those for the IL-anions, indicating that the IL-cations have stronger interactions with C₆₀ than the IL-anions. This also suggests that the π -cation interaction contributes more to mechanism of the C₆₀-IL interaction, compared with the π -anion interaction. Gao *et al.* also found that π -cation interaction can play a dominated role in the dispersion of multi-walled carbon nanotubes (CNTs) by in a IL-based polyether in aqueous solutions.¹⁹ As C₆₀ is non-polar, and ILs are polar molecules, the van der Waals interactions that are mainly dispersion and induction interactions also contribute to the mechanism in CNP-IL interactions.²⁴

The estimated quantum parameters for the C₆₀-IL complexes are presented in Table 1. For the C₆₀-[C_nmim][BF₄] complexes, the calculated *HF* values are negative, indicating that the formation of the complexes is exothermic. For the C₆₀-[C_nmim][Cl] and C₆₀-[C_nmim][PF₆] complexes, the calculated *HF* values are positive, indicating that the formation of the complexes is endothermic. In general, the *HF* values decrease with an increase of the alkyl side chain length on the imidazolium ring. The calculated *E*_{INT} values are negative, indicating that C₆₀ can form stable complexes with ILs. Generally, the alkyl side chain length on the imidazolium ring has no significant impacts on *E*_{INT} for the C₆₀-IL interactions. However, such cations of the general formula [C_nmim]⁺ studied contain both a symmetry-breaking region (*n*_C < 7) and hydrophobic region.²⁹ Moreover, CNPs exhibit extreme hydrophobicity.³⁰ Our previous study also indicates that hydrophobic interaction can provide a partial contribution to the mechanism for the C₆₀-IL interaction.³¹ According to the Mulliken population

Table 1. Estimated quantum parameters for the C₆₀-IL complexes

	Heat of formation (kcal/mol)	Interaction energies (kcal/mol)	Mulliken Charges (C ₆₀) <i>q</i> (e)
[C ₂ mim][BF ₄]	-397.1	-10.3	-0.0013
[C ₃ mim][BF ₄]	-401.5	-5.3	-0.0009
[C ₄ mim][BF ₄]	-410.2	-6.2	-0.0011
[C ₅ mim][BF ₄]	-412.8	-6.8	-0.0010
[C ₆ mim][BF ₄]	-417.7	-6.7	-0.0015
[C ₈ mim][BF ₄]	-429.2	-9.7	-0.0032
[C ₁₀ mim][BF ₄]	-439.9	-4.3	-0.0013
[C ₂ mim][Cl]	796.1	-3.4	-0.0003
[C ₃ mim][Cl]	789.4	-2.3	-0.0010
[C ₄ mim][Cl]	787.5	-5.5	-0.0015
[C ₅ mim][Cl]	775.3	0.5	-0.0006
[C ₆ mim][Cl]	775.9	-4.8	-0.0018
[C ₈ mim][Cl]	763.0	-2.2	-0.0003
[C ₁₀ mim][Cl]	754.0	-4.0	-0.0006
[C ₂ mim][PF ₆]	357.5	-0.1	-0.00004
[C ₃ mim][PF ₆]	380.4	-27.6	-0.0016
[C ₄ mim][PF ₆]	346.5	-2.9	-0.0004
[C ₅ mim][PF ₆]	343.1	-1.7	-0.0006
[C ₆ mim][PF ₆]	363.9	-28.3	-0.0009
[C ₈ mim][PF ₆]	325.8	-1.1	-0.0006
[C ₁₀ mim][PF ₆]	314.7	-1.2	-0.0006

analysis, C₆₀ has negative charges (*q*), implying that charge transfer occurred from IL to C₆₀ during the C₆₀-IL interaction, as indicated in Table 1. The results of Wagle *et al.* also suggested that the direction of charge transfer determined from a Mulliken population analysis is from IL to polyaromatic hydrocarbons (as precursors of C₆₀).³² In addition, it is noticeable that a weak correlation exists between the degree of charge transfer and the alkyl side chain length attached to the imidazolium ring.

Impacts of IL Alkyl Chain Length and C₆₀-IL Interactions on C₆₀ Dispersion in Bulk ILs. C₆₀-IL dispersions have been investigated by means of full atomistic MD simulations. Figure S6 (Supplementary data) presents snapshots corresponding to the dispersion state and spatial distribution of C₆₀ agglomerates in the different bulk ILs after 100,000 simulation steps. Though different dispersion extent can be obtained in the different bulk ILs, in general, C₆₀ can be effectively dispersed in the bulk ILs. As discussed above, there are special interactions such as π -cation and hydrophobic interaction between C₆₀ and ILs. When C₆₀ are ground with ILs, the strong π - π interaction between C₆₀ is shielded by ILs. Then these special interactions could be the driving force that disperses C₆₀ in the bulk ILs. Experimental studies of Wang *et al.* also suggest that ILs finely disperse single-walled CNTs by shielding a strong stacking interaction among CNPs.¹⁸

The evolution of the MSD of each system with the simulation time was shown in Figure S7 (Supplementary data). Furthermore, the number of carbon atoms in the alkyl chain of ILs is varied to probe its effects on the C₆₀ dispersion state

(Figure 2). For the $[\text{BF}_4]^-$ analog, the dispersion extent ($D_{\text{fullerene}}$) increases with an increase of the alkyl side chain length attached to the imidazolium ring. However, it is noted that, with a further increase of the alkyl side chain length, the dispersion extent of C_{60} decreases. This observation also implies that a good dispersion can be obtained by the presence of $[\text{C}_4\text{mim}][\text{BF}_4]$. Generally, for the $[\text{Cl}]^-$ and $[\text{PF}_6]^-$ analogs the increase in the alkyl side chain length decreases $D_{\text{fullerene}}$, indicating that a good dispersion can be obtained by the presence of short alkyl side chain. Note that IL contain-

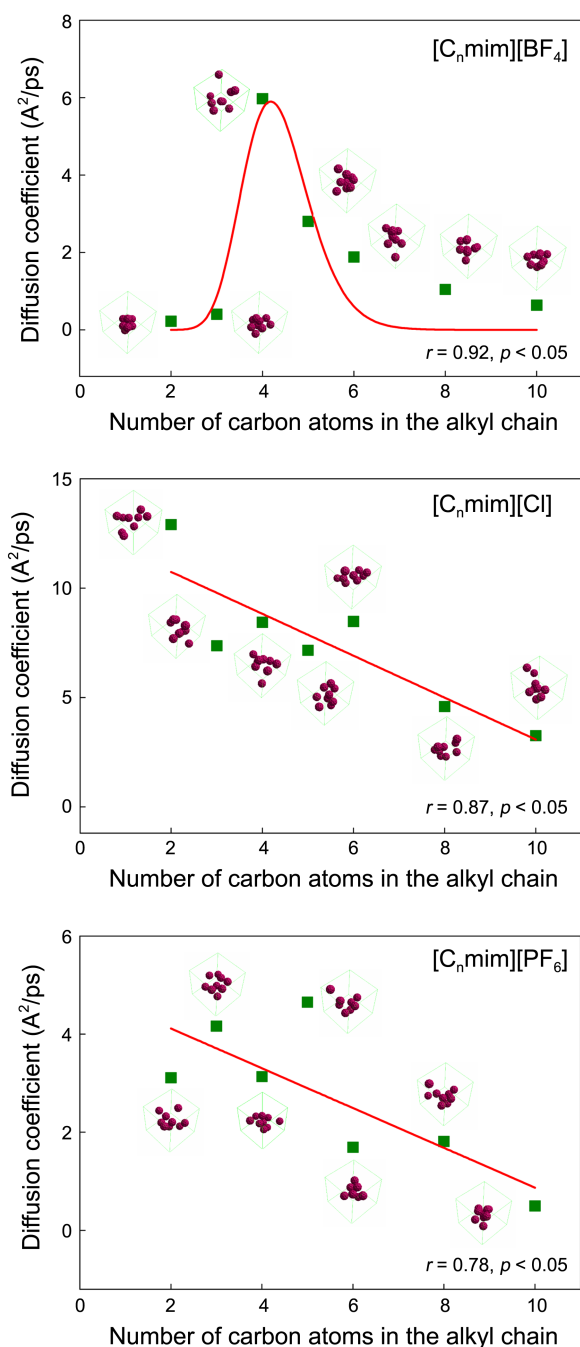


Figure 2. Diffusion coefficients of C_{60} as a function of the number of carbon atoms in the alkyl chain attached to the imidazolium ring. The insets are the perspective snapshots for the dispersion states of C_{60} in the different bulk ILs (not shown).

ing $[\text{BF}_4]^-$ exhibits a different effect from the other two ILs containing $[\text{Cl}]^-$ and $[\text{PF}_6]^-$. One can conclude that the anion may contribute to the effect. However, the anionic effect on the solubility of a solute is difficult to correlate.³³ As aforementioned, the thermodynamic condition for the formation of the C_{60} - $[\text{C}_n\text{mim}][\text{BF}_4]$ complexes is also different from the C_{60} - $[\text{C}_n\text{mim}][\text{Cl}]$ and C_{60} - $[\text{C}_n\text{mim}][\text{PF}_6]$ complexes. This implies that the thermodynamic property can play an important role in governing the effect of alkyl side chain length on the $D_{\text{fullerene}}$ values for the $[\text{BF}_4]^-$ analog. After a number of independent MD runs, note that ILs can influence the agglomeration behavior of C_{60} nanoparticles and cause their physical transformation. Thus we were able to expect that this finding may motivate new experimental studies on the assessment of ILs impacts on the environmental behavior of C_{60} . Song *et al.* found that C_{60} nanoparticles with smaller size may have higher toxicity potency. As this study showed that ILs generally probe to disperse the C_{60} agglomerates, the presence of ILs may enhance the toxicity of C_{60} nanoparticles.³⁴

The PLS regression technique was used to find the fittest descriptors for developing the models of quantitative assessment of $D_{\text{fullerene}}$ (Eqs. (5)-(7)). Based on the C_{60} -IL interactions, four interpretative descriptors (HF , E_{INT} , q and n_C) are tested during the development of the models. For C_{60} in the bulk $[\text{C}_n\text{mim}][\text{BF}_4]$, HF and n_C are the most significant descriptors correlating with the $D_{\text{fullerene}}$ values. For C_{60} in the bulk $[\text{C}_n\text{mim}][\text{Cl}]$, q and n_C are the most significant descriptors correlating with the $D_{\text{fullerene}}$ values. For C_{60} in the bulk $[\text{C}_n\text{mim}][\text{PF}_6]$, E_{INT} and n_C are the most significant descriptors correlating with the $D_{\text{fullerene}}$ values.

C_{60} in $[\text{C}_n\text{mim}][\text{BF}_4]$:

$$D_{\text{fullerene}} = -534.913 - 1.394 \cdot HF - 7.715 \cdot n_C$$

$$n = 7, r = 0.918, RMSE = 0.753, Q_{\text{CUM}}^2 = 0.708 \quad (5)$$

C_{60} in $[\text{C}_n\text{mim}][\text{Cl}]$:

$$D_{\text{fullerene}} = 7.377 - 2.051 \times 10^3 \cdot q - 0.466 \cdot n_C$$

$$n = 7, r = 0.963, RMSE = 0.524, Q_{\text{CUM}}^2 = 0.857 \quad (6)$$

C_{60} in $[\text{C}_n\text{mim}][\text{PF}_6]$:

$$D_{\text{fullerene}} = 6.789 - 3.927 \times 10^{-2} \cdot E_{\text{INT}} - 0.620 \cdot n_C$$

$$n = 7, r = 0.903, RMSE = 0.627, Q_{\text{CUM}}^2 = 0.592 \quad (7)$$

where n stands for the number of ILs, r is coefficient of correlation, $RMSE$ is root mean squared error, and Q_{CUM}^2 is the cumulative percentage of variance explained for extracted components. Q_{CUM}^2 of the models are higher than 0.5, suggesting that their good robustness and internal predictability. Thus the models have high goodness-of-fit. The dispersion extent of C_{60} is related to three molecular descriptors (HF , E_{INT} , and q) that describe the C_{60} -IL interactions. It is well known that within a particular family of chemical compounds (*e.g.* IL) that there are strong correlations between structure and observed properties.^{17,35} Thus, it is reasonable to believe that the molecular structural characteristics govern the $D_{\text{fullerene}}$ values.

Conclusion

Through a detailed simulation at different theoretical levels (QM, MM, and classical MD), we have mainly addressed the dispersion mechanism of C₆₀ agglomerates in the imidazolium-based ILs of varying the alkyl side chain lengths and anionic types. The IL-cation has a stronger interaction with C₆₀ than its anionic partner. The formation of the C₆₀-[C_nmim][BF₄] complexes is exothermic; the formation of the C₆₀-[C_nmim][Cl] and C₆₀-[C_nmim][PF₆] complexes is endothermic; and C₆₀ can form stable complex with each IL molecule. Furthermore, charge transfer occurred from IL to C₆₀ during the C₆₀-IL interaction. The models on D_{fullerene} developed by PLS show high goodness-of-fit and robustness. Three molecular features (*HF*, *E*_{INT}, and *q*) that describe the C₆₀-IL interaction and the alkyl side chain lengths attached to the imidazolium ring were found to be the decisive factors controlling D_{fullerene}.

Acknowledgments. The study was supported by the Project Funded by the Priority Academic Program Development of Jiangsu Higher Education Institutions (PAPD), the Foundation Research Project of Jiangsu Province (Grant No. BK20140987), and the Natural Science Key Research of Jiangsu Province High Education (Grant No. 11KJA170002). Degao Wang also thanks the support from “Open fund by Jiangsu Key Laboratory of Atmospheric Environment Monitoring and Pollution Control (Grant No. KHK1309)”. We thank the reviewers for their valuable comments on the manuscript.

References

- Petersen, E. J.; Zhang, L.; Mattison, N. T.; O'Carroll, D. M.; Whelton, A. J.; Uddin, N.; Nguyen, T.; Huang, Q.; Henry, T. B.; Holbrook, R. D.; Chen, K. L. *Environ. Sci. Technol.* **2011**, *45*, 9837.
- Sanchis, J.; Berrojalbiz, N.; Caballero, G.; Dachs, J.; Farré, M.; Barceló, D. *Environ. Sci. Technol.* **2012**, *46*, 1335.
- Cohen, Y.; Rallo, R.; Liu, R.; Liu, H. H. *Acc. Chem. Res.* **2013**, *46*, 802.
- Klaine, S. J.; Koelmans, A. A.; Horne, N.; Carley, S.; Handy, R. D.; Kapustka, L.; Nowack, B.; von der Kammer, F. *Environ. Toxicol. Chem.* **2012**, *31*, 3.
- Lowry, G. V.; Gregory, K. B.; Apte, S. C.; Lead, J. R. *Environ. Sci. Technol.* **2012**, *46*, 6893.
- Li, Q.; Xie, B.; Hwang, Y. S.; Xu, Y. *Environ. Sci. Technol.* **2009**, *43*, 3574.
- Wang, L.; Huang, Y.; Kan, A. T.; Tomson, M. B.; Chen, W. *Environ. Sci. Technol.* **2012**, *46*, 5422.
- Tummala, N. R.; Morrow, B. H.; Resasco, D. E.; Striolo, A. *ACS Nano* **2010**, *4*, 7193.
- Hou, L.; Zhu, D.; Wang, X.; Wang, L.; Zhang, C.; Chen, W. *Environ. Toxicol. Chem.* **2013**, *32*, 493.
- Chang, X.; Vikesland, P. J. *Environ. Pollut.* **2009**, *157*, 1072.
- Xie, B.; Xu, Z.; Guo, W.; Li, Q. *Environ. Sci. Technol.* **2008**, *42*, 2853.
- Chen, K. L.; Elimelech, M. *J. Colloid. Interface Sci.* **2007**, *309*, 126.
- Lin, S.; Blankschtein, D. *J. Phys. Chem. B* **2010**, *114*, 15616.
- Li, D.; Lyon, D. Y.; Li, Q.; Alvarez, P. J. *Environ. Toxicol. Chem.* **2008**, *27*, 1888.
- Binnemans, K. *Chem. Rev.* **2007**, *107*, 2592.
- Pham, T. P.; Cho, C. W.; Yun, Y. S. *Water Res.* **2010**, *44*, 352.
- Haumann, M.; Riisager, A. *Chem. Rev.* **2008**, *108*, 1474.
- Wang, J.; Chu, H.; Li, Y. *ACS Nano* **2008**, *2*, 2540.
- Gao, H.; Zhang, S.; Huang, D.; Zheng, L. *Colloid. Polym. Sci.* **2012**, *290*, 757.
- Maciel, C.; Fileti, E. E. *Chem. Phys. Lett.* **2013**, *568-569*, 75.
- Ge, H. L.; Liu, S. S.; Zhu, X. W.; Liu, H. L.; Wang, L. *J. Environ. Sci. Technol.* **2011**, *45*, 1623.
- Markiewicz, M.; Jungnickel, C.; Arp, H. P. *Environ. Sci. Technol.* **2013**, *47*, 6951.
- Zou, M.; Zhang, J.; Chen, J.; Li, X. *Environ. Sci. Technol.* **2012**, *46*, 8887.
- Sun, Q.; Xie, H. B.; Chen, J.; Li, X.; Wang, Z.; Sheng, L. *Chemosphere* **2013**, *92*, 429.
- Wang, Z.; Chen, J.; Sun, Q.; Peijnenburg, W. J. G. M. *Environ. Int.* **2011**, *37*, 1078.
- Westerhoff, P.; Nowack, B. *Acc. Chem. Res.* **2013**, *46*, 844.
- Santos, S. G.; Santana, J. V.; Maia, F. F., Jr.; Lemos, V.; Freire, V. N.; Caetano, E. W.; Cavada, B. S.; Albuquerque, E. L. *J. Phys. Chem. B* **2008**, *112*, 14267.
- Puzyn, T.; Rasulev, B.; Gajewicz, A.; Hu, X. K.; Dasari, T. P.; Michalkova, A.; Hwang, H. M.; Toropov, A.; Leszczynska, D.; Leszczynski, J. *Nat. Nanotechnol.* **2011**, *6*, 175.
- Pinkert, A.; Marsh, K. N.; Pang, S.; Staiger, M. P. *Chem. Rev.* **2009**, *109*, 6712.
- Yang, K.; Xing, B. *Chem. Rev.* **2010**, *110*, 5989.
- Wang, Z.; Tang, L. L.; Peijnenburg, W. J. G. M. *Environ. Toxicol. Chem.* **2014**, *33*, 1802.
- Wagle, D.; Kamath, G.; Baker, G. A. *J. Phys. Chem. C* **2013**, *117*, 4521.
- Stark, A. *Top. Curr. Chem.* **2010**, *290*, 41.
- Song, M.; Yuan, S.; Yin, J.; Wang, X.; Meng, Z.; Wang, H.; Jiang, G. *Environ. Sci. Technol.* **2012**, *46*, 3457.
- Pádua, A. A.; Costa Gomes, M. F.; Canongia Lopes, J. N. *Acc. Chem. Res.* **2007**, *40*, 1087.